

The Permeability of Whole and Jointed Barre Granite

R. L. KRANZ*†
A. D. FRANKEL*†
T. ENGELDER*
C. H. SCHOLZ*†

The permeability of whole and jointed Barre granite was measured at pressures up to 2 kbars. Jointed samples were actually split cylinders joined by surfaces with controlled surface roughness. Samples with induced tension fractures were also measured. The permeability of the whole rock ranged from about 10^{-6} to 10^{-7} darcies. The permeability of the jointed rock ranged from about 8×10^{-5} darcies at low pressure down to that of the whole rock at high pressures. Permeability was not a simple function of the difference between external confining pressure (P_c) and internal fluid pressure (P_f). Changes in permeability were found to be proportional to $(b dP_f - a dP_c)$ where $b/a < 1$ for the jointed rock and $b/a \approx 1$ for whole rock. The order of application of P_c and P_f was also important. Permeability hysteresis and an ultimate decrease in permeability in both whole and jointed rock resulted when internal fluid pressure was cycled. This effect seems to diminish with increasing confining pressure. At a particular P_c , the volume flow rate, q , is proportional to $(P_c - P_f)^{-n}$. Increasing the surface roughness of the joints decreased the value of n , which was smallest for the tension fracture and the whole rock. Within the uncertainty of joint aperture measurements, a flat plate model of the joint seem inadequate.

INTRODUCTION

As part of a larger study designed to investigate the effects of joint roughness, geometry and filling on fluid flow at geologic pressures and temperatures, we report here initial results on Barre granite. Specifically, we measured the permeability of whole and jointed Barre granite at room temperature and pressures up to 2 kbars. Jointed samples were of two kinds: split cylinders joined by surfaces with controlled surface roughness and cylinders with artificially induced tension fractures. Some of our results corroborate previous investigations, but we have also determined that the stress history and joint surface roughness have a large effect on the hydraulic properties of rock and, as this has rarely been specifically taken into account, is, we feel, of major importance.

Data on the permeability of low porosity, crystalline rock are scarce. Westerly granite is the only rock that has been extensively investigated. Brace *et al.* [1]

reported on the permeability of Westerly granite as a function of effective stress (commonly taken as the difference between the external confining pressure and internal fluid pressure), Zoback & Byerlee [2] investigated the effect of deviatoric stress on the permeability of Westerly granite, and Summers *et al.* [3] described permeability changes in Westerly granite at temperatures between 100° and 400°C. With one exception, [3], all measurements were on whole, unjointed rock. The permeability of jointed granite has been measured *in situ* by Pratt *et al.* [4] and in a large granite core by Witherspoon *et al.* [5]. Both studies were restricted by sample size to stresses below 300 bars†.

Brace [6] has concisely summarized the results from the literature dealing with the permeability of geologic materials. The following points are worth repeating: (1) stress produces large changes in permeability, both increases and decreases, in all porous material but joints are extremely sensitive to stress changes relative to the surrounding whole rock; (2) the permeability of jointed rock is several orders of magnitude greater than that of intact rock (at least over the stress range measured); (3) the simple effective stress law of confining pressure minus pore pressure may be adequate for unjointed granite, is not adequate for sandstones and

* Lamont-Doherty Geological Observatory of Columbia University, Palisades, NY 10964, U.S.A.

† Also, at the Dept. of Geological Sciences, Columbia University.

‡ 1 bar = 10^5 N/m² = 0.1 MPa.

there are not yet enough data to even test it for jointed rock.

SAMPLE PREPARATION

Whole samples

All cores, approximately 3.5 cm in diameter and 9 cm in length were taken in the same direction from a single block of Barre granite. Their ends were surface ground parallel to within 0.001 cm from side to side.

Split samples

Another block of Barre granite was saw-cut into large prismatic sections with ground sides. Two sections with parallel sides were clamped together and cores, also approximately 3.5 cm in diameter, were taken centered on the joint between the sections. These split, cylindrical samples were then re-clamped and saw-cut to be approximately 9 cm in length. The ends were ground parallel like the whole samples. The split samples were then unclamped and the interior, opposing surfaces were ground with number 120 grit. Some samples were subsequently ground with number 600 grit and others further polished with Linde 0.3 μ alumina polishing compound. All surfaces were prepared, stored and protected in pairs.

For our *tension fracture* samples, two grooves, approximately 1 mm in depth, were made 180° apart down the length of several of the whole samples. They were then placed between two V-shaped anvils and split from groove to groove as in a Brazilian strength test.

PROCEDURE

Experiments were conducted in a triaxial, servo-controlled, hydraulic press equipped with a 5.08 cm bore pressure vessel. Kerosene was used as the pressure medium as well as the fluid pumped through the rock. It is chemically inert with respect to the rock so we are looking at mechanical effects of pressure only. The confining pressure system was independently controlled and separate from the internal fluid system.

All whole samples were covered with a thin copper jacket. Steel end caps with center holes and radial grooves were affixed to the whole samples. To permit fluid access to the entire end surface of the sample, a thin layer of grit from a pulverized grinding wheel was placed between the sample and each end cap. A steel piston was affixed to one side of this assembly and the pressure vessel closure to the other. Fluid could be admitted or withdrawn through central ports in the piston and top closure.

Strain gauges were cemented to the copper jacket in an array which permitted strain to be measured at a number of points along the length of the sample.

Split cylinder assemblies were made in the same way except the layer of grit was omitted and the samples were jacketed with polyolethane.

To measure joint aperture changes, a four-armed

cantilever device was used (Fig. 1). It consisted of four thin, rectangular beryllium-copper beams connected in a radially symmetric pattern to an aluminum ring which was slipped over the sample. A certain amount of tension kept pads at the end of each arm firmly pressed against the sample. Each arm had an electric resistance strain gauge on it. It was arranged on the sample so that two of the arms measured the sum of joint closure and rock compression, and the other two measured rock compression only. The output of one pair was subtracted electrically from the output of the other pair so that the result was proportional to the joint closure. The dilatometer was calibrated against a micrometer. The effect of pressure on the dilatometer was also measured and taken into account.

Both confining pressure and internal fluid pressure were measured outside the pressure vessel in two ways. For recording, we used the output from two high pressure BLH, Inc. pressure transducers. In addition, we visually monitored confining pressure with a Heise gauge and internal fluid pressure with two Heise gauges connected within the system above and below the sample column. A differential pressure transducer capable of detecting differences of 0.1 bars under ambient pressures as high as 3 kbars was also connected between the top and bottom of the sample column. Schematically, our pore pressure system is similar to that shown in [2].

Permeability measurements were made with a procedure which closely follows that of Brace *et al.* [1]. A similar procedure has been used by Zoback & Byerlee [2]. Briefly, a pressure step (about 5–10 bars) much smaller than the ambient pore pressure was introduced to either the top or bottom of the sample column assembly and the decay in the pressure head was monitored with the differential pressure transducer. The pulse decays in time according to the equation

$$P = P_0 e^{-\alpha t} \quad (1)$$

with

$$\alpha = \frac{kA(V_2 + V_1)}{\beta\mu LV_2V_1} \quad (2)$$

where k is the permeability, A is the cross section through which fluid flows, β is the isothermal compressibility of the fluid, μ is the dynamic viscosity, L is the sample length and V_1 and V_2 are the volumes of pore fluid reservoirs at the top and bottom of the sample, respectively. For our system, $V_1 = 20 \text{ cm}^3$, $V_2 = 15 \text{ cm}^3$, $L = 9 \text{ cm}$, $A = 9.6 \text{ cm}^2$ for the whole rock samples. Isothermal compressibility and dynamic viscosity of kerosene as a function of pressure can be found in [7] and [8], respectively. Once α is evaluated from the pulse decay curve, equation (2) can be used to calculate the permeability for the whole rock.

This method assumes that Darcy's law holds. That is

$$q = \frac{kA}{\mu} \frac{dP}{dL} \quad (3)$$

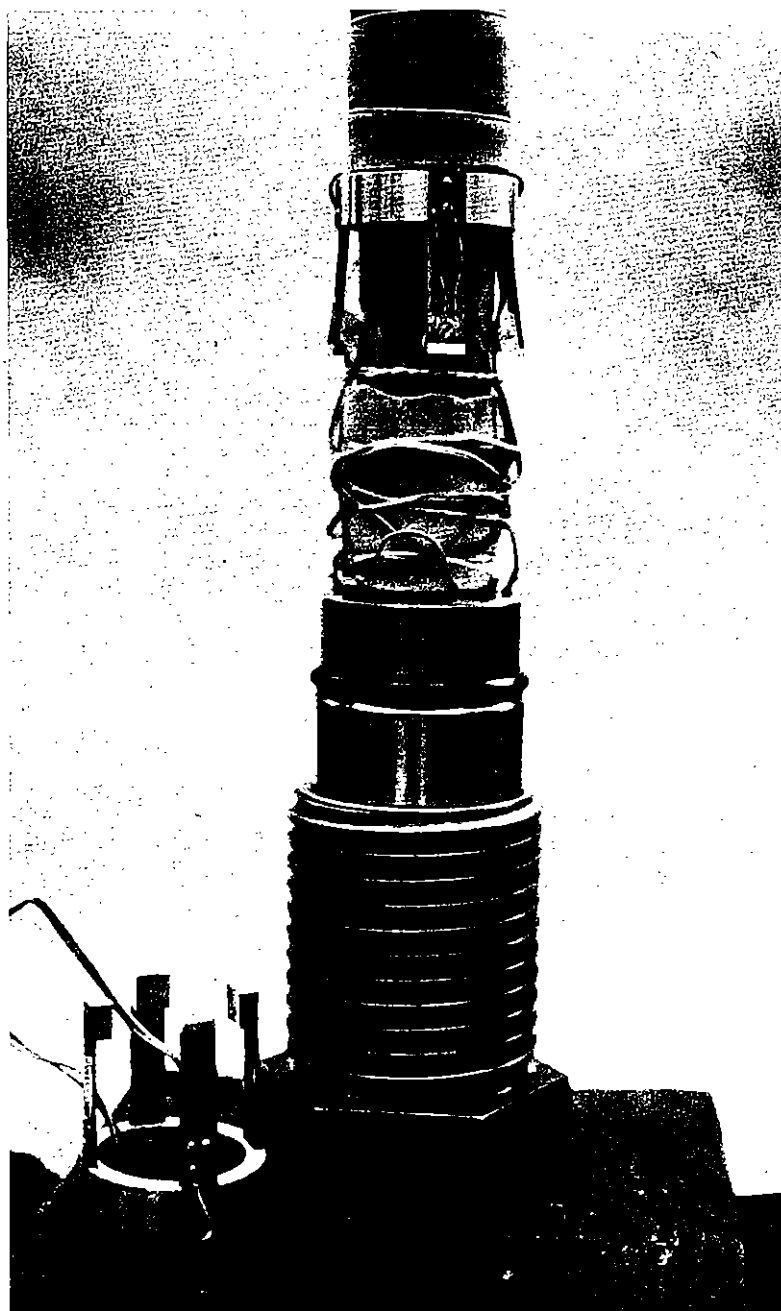


Fig. 1. Sample column assembly showing four-armed dilatometer around sample. A second dilatometer can be seen at the base of the column.

where q is the volume flow rate. It also assumes that a linear pressure gradient exists along the length of the sample.

The same procedure was used for all split cylinder samples. This allows a direct comparison between whole rock and rock with a joint, but will not give an absolute value of permeability for the joint itself because the assumptions made in deriving (2) do not necessarily apply to joints.

Joints are often approximated as a parallel plate opening, for which [5,9,10] the volume flow rate per plate width is

$$q = \frac{d^3}{12\mu} \frac{dP}{dL} \quad (4)$$

where d is the plate opening. Comparing (3) and (4), a single joint permeability may be defined as

$$k_j = d^2/12 \quad (5)$$

One can modify (2) by taking A , the cross section exposed to the fluid, to be simply the joint opening d times the cylinder diameter (3.5 cm). Permeability calculated in this fashion for the joint alone can be compared to permeability calculated using (5) if the absolute value of d is known. Differences in the two calculations will be, in a sense, a measure of the deviation of the actual joint from the flat plate model. Implicit in this modification is an assumption that essentially all flow occurs through the joint. This may not be the case for rock with higher porosities than that

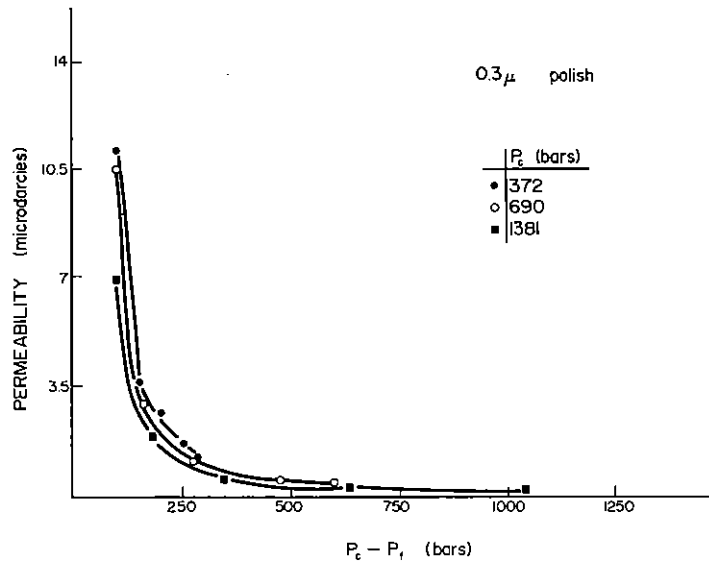


Fig. 3. Permeability at various pressures of jointed Barre granite with joint surfaces prepared with 0.3 μ alumina polish.

The following details should be noted. At a particular value of $P_c - P_f$, the higher the P_c value the lower the permeability. This is particularly striking for the 120 grit surface and becomes less marked as the surface becomes smoother. The rate of change of permeability with changing $P_c - P_f$ is greatest at low pressure and decreases almost to zero at high pressure. The rougher the joint surface, the slower the decline of permeability with increasing $P_c - P_f$.

The data in Fig. 6, which are for a tension fracture, were collected following the procedure of Fig. 2b. The hysteresis is quite apparent for this rough joint surface. At any particular confining pressure, lowering the internal fluid pressure (raising $P_c - P_f$) resulted in a decrease in permeability which was not entirely recovered when the internal fluid pressure was raised to its initial value. Note that the hysteresis decreases as the confining pressure is increased. Part of this decrease is un-

doubtedly due to cycling alone. At 2 kbars of confining pressure there was almost no hysteresis and the permeability was almost constant above the 500 bar value of $P_c - P_f$.

The permeability of the whole rock as a function of $P_c - P_f$ is shown in Fig. 7. Note that the permeability is on the order of a microdarcy or less at high pressures. Measurements were made following the procedure of Fig. 2a in most cases. The results of 3 hysteresis tests following the procedure of Fig. 2b are also given. The open symbols represent initial permeabilities before pore pressure was dropped. The closed symbol directly beneath each open symbol represents the permeability after pore pressure was raised to its initial value. As in the tension fracture, the difference between the two seems to decrease with increasing confining pressure.

From equation (3) we note that the volume flow rate q is proportional to kA , which may be calculated using (2) once α is measured. A direct comparison between the whole rock and each jointed rock sample can be

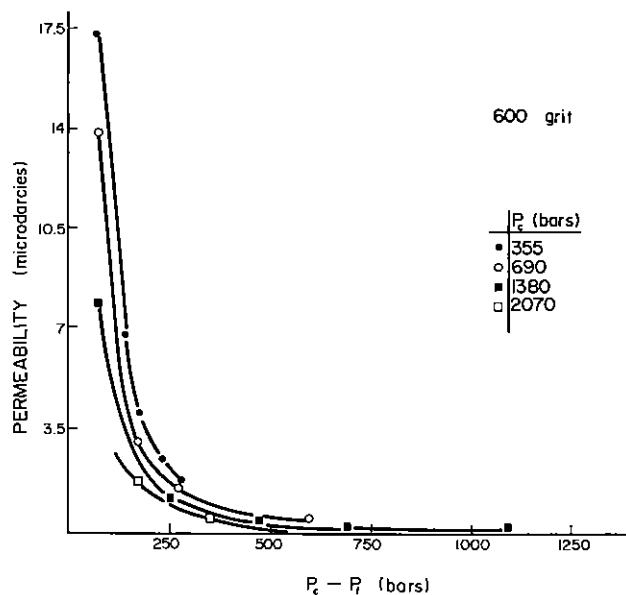


Fig. 4. Permeability at various pressures of jointed Barre granite with joint surfaces ground with number 600 grit.

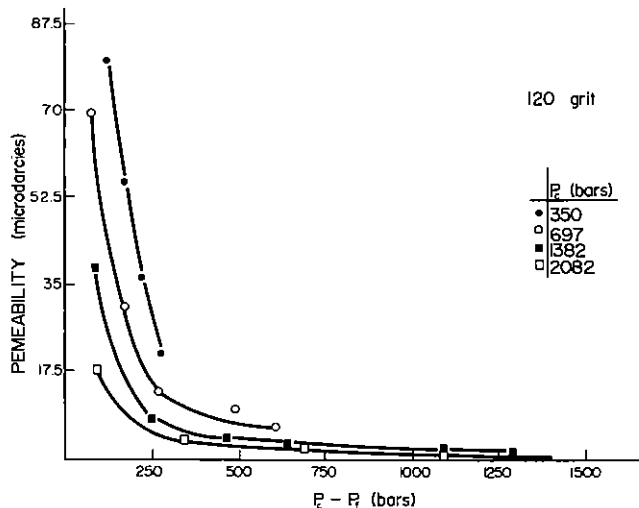


Fig. 5. Permeability at various pressures of jointed Barre granite with joint surfaces ground with number 120 grit.

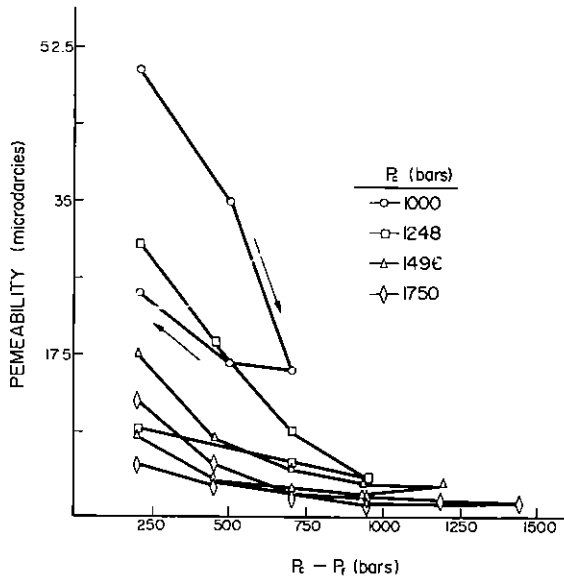


Fig. 6. Permeability at various pressures of Barre granite with a tension fracture, measured using the procedure of Fig. 2b.

made using kA rather than k . This eliminates any questions about what value one should take for A for the jointed sample. Because of the stress history effect, comparisons should be limited to measurements at the same P_c or P_f . We fit kA to an equation of the form

$$kA = [kA]_0 ([P_c - P_f]^{-n}) \quad (6)$$

By plotting $\log [kA]$ vs $\log [P_c - P_f]$ we find n . Figure 8 gives an example for the jointed rock samples at $P_c = 690$ bars. Table 1 lists the values of n at various pressures for all available data. Two things become immediately apparent. First, as confining pressure is raised, all samples show a decreasing dependency on $P_c - P_f$. Also, as mentioned previously, the rougher the surface the smaller the pressure effect at all pressures. It should also be noticed that since the n values for the jointed rock samples are greater than for the whole rock, the curves will intersect at some $P_c - P_f$ value. That is, at some pressure there will be no apparent difference in the flow rate between a rock with a joint and an unjointed rock. For the sample with the smoothest joint surface this projected pressure is between 2 and 3 kbars. For the roughest joint surface it is between 10 and 15 kbars. Obviously, such a projection ignores the effects of temperature and other natural variables.

As mentioned previously, using the dilatometer to measure the joint aperture at the same time that permeability is being measured offers the opportunity to evaluate the flat plate model of a joint. If one assumes that the joint aperture alone is the effective cross sectional area to which fluid is exposed, then in equation (2), A equals 3.5 cm times the joint opening (d). We found, for example, that the joint with surfaces prepared with 120 grit could be squeezed down about 36 μm . From the change of aperture with pressure we estimated the maximum joint closure possible to be about 40 μm . Using this value for d at zero pressure,

we calculated the permeability of the joint alone. In Fig. 9 we compare this with the flat plate model (equation 5). Data collected are given in Table 2. Uncertainty in d is about 1 μm .

Data points 1 through 6 in Table 2 indicate how rapidly the joint closes down as confining pressure is raised. Data points 7 through 13 show that with the introduction of internal fluid pressure the joint recovers most, but not all, of the aperture closure produced by an equivalent value of $P_c - P_f$ (compare data points 5 and 8, for example). Permeability measurements were made starting at the conditions of data point 14. Confining pressure was raised and, after data point 21, internal fluid pressure was raised until near the value of P_c . After data point 26, P_f was lowered and a second cycle begun.

It is apparent from Fig. 9 that, within the uncertainty of the aperture measurements, a flat plate does not adequately model this joint. The flat plate model predicts permeabilities and orders of magnitude higher than determined. The model also does not consider the stress history. The joint apparently suffers enough damage during the first cycle of measurements (data points 1 through 26 in Table 2) that it no longer responds in the predicted way. During the second cycle (after data point 27 in Table 2), permeability is significantly lower than during the first cycle, even though the measured apertures are about the same. Once the joint has been squeezed down, the two sides tend to remain close together until the internal fluid pressure is raised to a substantial percentage of the external confining pressure, after which the aperture opens rapidly (compare data points 7–13 and 21–26). The phenomenon of the joint being wedged open by high internal fluid pressure requires more clarification and is under current investigation.

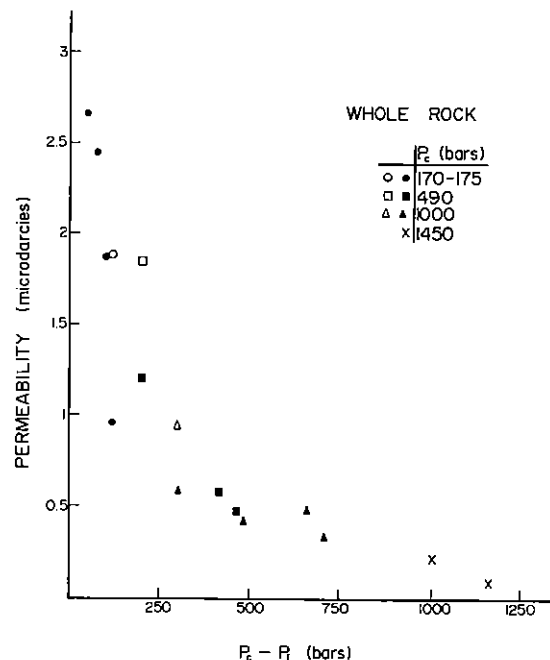


Fig. 7. Permeability of whole, unjointed Barre granite at various pressures. Open symbols and closed symbols directly beneath them are beginning and end points of cyclic experiments following the procedure of Fig. 2b.

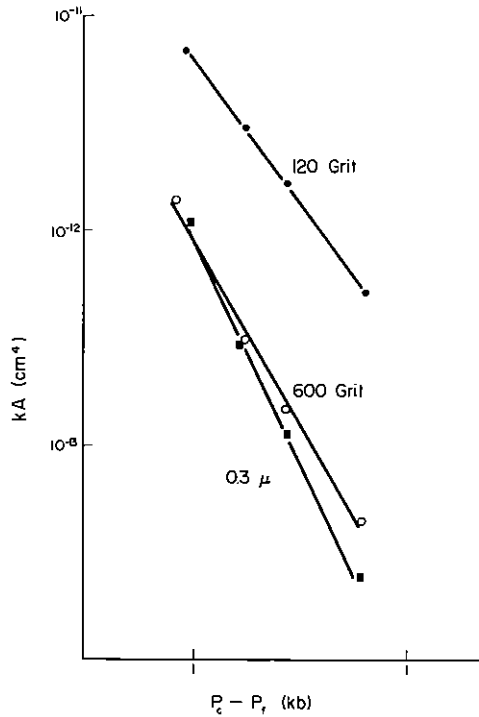


Fig. 8. Permeability times cross-sectional area (kA) as a function of $P_c - P_f$ (with P_c held constant at 690 bars) for different jointed samples.

DISCUSSION

Effective stress

Permeability k is a function of many variables, the most important of which are evidently confining pressure, internal fluid pressure, temperature, and in the case of joints, surface roughness. Unfortunately, k does not appear to be simply proportional to $P_c - P_f$. When one of these pressures is held constant and the other is changed two things become apparent. First, the relative effects on the change of permeability are not always equal for equal changes in P_c and P_f and second, the order in which the two pressures are varied also has an effect on the permeability. That is, k is stress history-dependent.

Suppose k to be a function only of P_c and P_f . Then we may write

$$\begin{aligned}
 dk &= \left[\frac{\partial k}{\partial (P_c - P_f)} \right]_{P_f} d(P_c - P_f) + \left[\frac{\partial k}{\partial (P_c - P_f)} \right]_{P_c} d(P_c - P_f) \\
 &= \left[\frac{\partial k}{\partial (P_c - P_f)} \right]_{P_f} dP_c - \left[\frac{\partial k}{\partial (P_c - P_f)} \right]_{P_c} dP_f \\
 &= -a dP_c + b dP_f. \tag{7}
 \end{aligned}$$

From this we see that the coefficients a and b give the relative effects of confining and internal fluid pressure changes. They are the slopes of equal P_f and equal P_c lines on a permeability vs $P_c - P_f$ graph. When P_c and P_f are changed by equal amounts, the value of $b - a$ is proportional to the change in k . For example, if both P_c and P_f are increased by δ , then $dk = (b - a)\delta$. If dk is positive (permeability increases)

then b is greater than a and internal fluid pressure is evidently of greater importance than confining pressure. This, as we have shown, is decidedly not the case for jointed Barre granite. Permeability was less at higher confining pressures when compared at the same $P_c - P_f$ value (e.g. $b/a < 1$). Zoback [12] found $2.2 < b/a < 4$ for several unjointed sandstone. That is, P_f had a greater effect than P_c . Bracc *et al.* [1] implied that a simple effective stress law of $(P_c - P_f)$ held for Westerly granite. This is equivalent to having $b/a = 1$. For whole Barre granite b/a is also close to one but we hesitate to try and assign a value because it is apparent that b/a is stress history dependent. In addition, for joints b/a is apparently also a function of surface roughness and the ambient pressure.

Taking all of this into account, we conclude that there is no simple effective stress law for the permeability of jointed rock. We have purposely avoided using the term 'effective stress' for this reason and because no effective stress law has yet to be developed which accounts for stress history dependence.

Surface roughness

The more highly polished a surface is the smaller the mean asperity height. In this sense, grinding has the same effect as normal pressure. For any particular initial statistical roughness, the greater the pressure, the greater the real area of contact with the opposing surface. Similarly, at any particular normal pressure, we would expect more real area of contact the less rough or more highly ground the two opposing surfaces are.

Asperities in contact affect permeability in two direct ways. They change the path length or tortuosity of flow path and they inhibit joint closure. Joint permeability defined by equation (5) does not take this into account. The effect of surface roughness can easily be seen by comparing Figs 3, 4, and 5. The highly polished surface (Fig. 3) most closely resembles a flat plate. Asperities are small so the joint closes rapidly at low pressures until enough of these asperities make contact with the

TABLE 1. DEPENDENCE OF kA ON $P_c - P_f$

$$\mu q \left[\frac{dP}{dL} \right]^{-1} = kA = [kA]_0 [(P_c - P_f)^{-n}]$$

P_c (bars)	Joint surface	kA_0^*	$n \pm 0.2$
350	120 grit	12.3	1.6
355	600 grit	1.2	1.9
372	0.3 μ polish	1.2	2.4
697	120 grit	7	1.3
690	600 grit	0.9	1.7
690	0.3 μ polish	0.9	2.1
1382	120 grit	3.3	1.2
1380	600 grit	0.5	1.5
1381	0.3 μ polish	0.7	2.1
2082	120 grit	1.1	0.8
2070	600 grit	0.4	1.5?
1000	tension fracture	60	1.3
1248	tension fracture	25	1.1
1496	tension fracture	10	1.0
1750	tension fracture	?	?
170-175	whole rock	1	0.9
1000	whole rock	0.65	0.8

* $\times 10^{-12} \text{ cm}^2$; $[kA]_0 = kA$ at $P_c - P_f = 100$ bars.

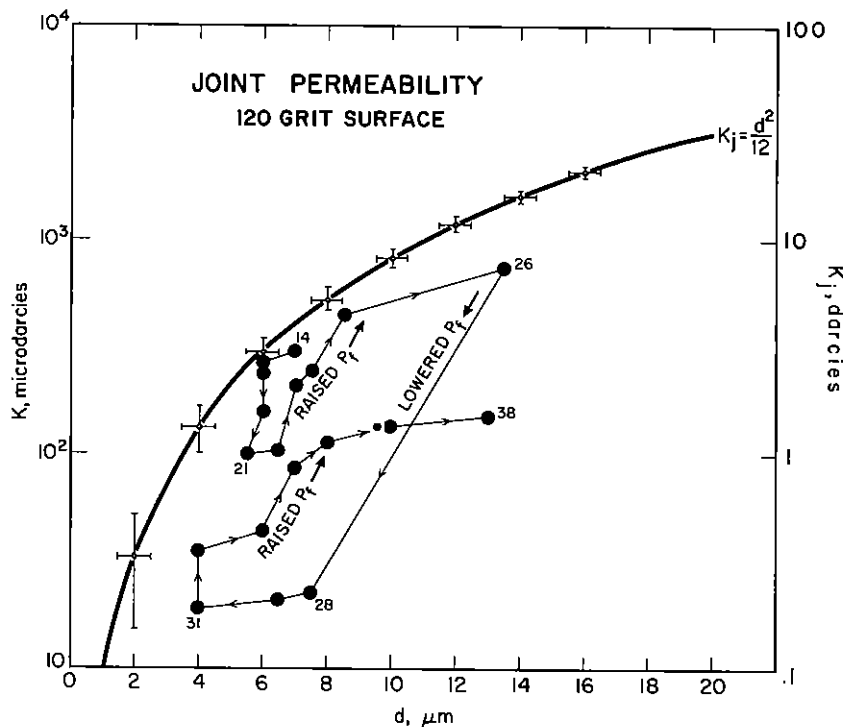


Fig. 9. Permeability of the joint alone as a function of joint aperture. K_j is the theoretical value assuming a flat plate model. Data points taken from Table 2.

opposing surface to increase the flow tortuosity and decrease the closure rate. Contrast this with Fig. 5 where the asperities are larger and tend to prop the joint open, thereby diminishing the rate of permeability decline as pressure is raised. Figure 4 shows intermediate behavior.

Iwai [13] has investigated the effects of contact area and asperity geometry on permeability. He found that at low pressure (2.6 bars) the real area of contact of a granite was less than 0.1% of the apparent total area and increased to 10–20% at 200 bars. He found a relation of the form

$$\gamma \frac{k}{k_0} + 1 = \frac{\psi}{\gamma A_r/A + 1} \quad (8)$$

where γ and ψ are empirical constants, k_0 is the zero pressure permeability, A_r is the real area of contact and A is the apparent joint surface area.

Though we have no data for the relationship between $P_c - P_f$ and A_r/A , Iwai [13] claims that the contact area increases linearly with normal load. This is consistent with the results of Bowden & Tabor [14] who show that, neglecting time effects,

$$A_r = N/h \quad (9)$$

where N is the average normal load on an asperity and h is the indentation hardness for the asperity material.

Consider the model of a part of a joint sketched in Fig. 10. Confining pressure acts on the entire joint surface area A . Equilibrium demands that

$$P_c A = N + P_f (A - A_r) \quad (10)$$

TABLE 2. JOINT APERTURE AND PERMEABILITY CHANGES FOR SAMPLE WITH 120 GRIT SURFACE

Data Pt.	P_c (bars)	P_f	d (μm)	K (microdarcies) ($\times 1$)	$K_j = d^2/12$ ($\times 10^4$)
1	0	0	40		
2	10	0	19		
3	20	0	16		
4	40	0	12		
5	75	0	9		
6	150	0	7		
7	300	55	4.5		
8	300	150	5.5		
9	300	205	7		
10	300	255	9.5		
11	300	265	10.5		
12	300	275	11.5		
13	300	285	13.5		
14	300	205	7	~300	408
15	500	205	6	~275	300
16	700	205	6	~260	300
17	1000	205	6	248	300
18	1200	205	6	243	300
19	1400	205	6		
20	1400	100	6	159	300
21	1400	50	5.5	98	252
22	1400	350	6.5	105	352
23	1400	600	7	210	408
24	1400	850	7.5	239	468
25	1400	1100	8.5	455	602
26	1400	1350	13.5	~750	1518
27	1400	200	7.5		
28	1700	230	7.5	22	468
29	2165	230	7.0	23	408
30	2700	230	6.5	21	352
31	3435	230	4	19	133
32	2735	230	4	21	133
33	2100	230	4	35	133
34	1425	230	6	44	300
35	1425	430	7	88	408
36	1455	985	8	103	533
37	1455	1275	10	135	833
38	1455	1395	13	149	1400

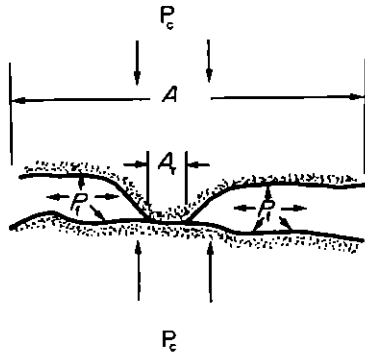


Fig. 10. An idealized joint section with an asperity subjected to external, P_c , and internal, P_f , pressures.

Substituting for N from (9) we get

$$\frac{A_r}{A} = \frac{P_c - P_f}{h - P_f} \quad (11)$$

To determine whether P_c or P_f has a greater effect on A_r , we compare

$$\frac{1}{A} \left[\frac{\partial A_r}{\partial P_c} \right]_{P_f} = \frac{1}{h - P_f}$$

and

$$\frac{1}{A} \left[\frac{\partial A_r}{\partial P_f} \right]_{P_c} = \frac{P_c - h}{[h - P_f]^2}$$

We see that

$$\left[\frac{\partial A_r}{\partial P_c} \right]_{P_f} > \left[\frac{\partial A_r}{\partial P_f} \right]_{P_c}$$

whenever $P_c + P_f < 2h$.

This condition is certainly met for all of our experiments so we conclude that the confining pressure will have a greater effect on the real area of contact than the internal fluid pressure. This simple model is therefore compatible with our experimental results. It is clear from Table 1, however, that changes in joint surface topography with normal stress are much more complicated than we have supposed. We have initiated a program to measure these changes in order to better understand the physics of joint deformation.

Whole rock

The absolute values of permeability for Barre granite are about a factor of 3 higher than those reported by Brace *et al.* [1] for Westerly granite over the pressure range measured here. The average grain size of Barre granite is about a factor of 2 greater than that for Westerly granite. In addition, Barre granite has a strong fabric because of a preferred crack orientation [15]. Our whole rock cores were oriented so that flow was forced along the rift-grain plane. These two factors probably account for the differences in permeability.

Stress history

Unrecovered permeability changes for jointed crystalline rock have been observed in the laboratory [5,13,17] and joint closure hysteresis has been observed [4] in the field. These were a result of cycling

the external normal stress. Since overburden pressures generally remain constant while internal fluid pressures change in natural rock systems, our method of demonstrating permeability hysteresis by cycling the internal pressure is preferable.

Witherspoon *et al.* [5] observed that flow rates showed a considerable difference between injection and withdrawal of fluid, but that the difference decreased with increasing normal stress. No significant permeability losses were observed by Zoback [12] when pore pressure was raised, then lowered in sandstone. We observed permeability hysteresis in jointed samples and whole rock when the internal fluid pressure was first lowered, then raised to its initial value (Figs 6 and 7). This hysteresis also seemed to decrease with increasing confining pressure.

Since hysteresis occurs in joint closure with a considerable non-recoverable part, some asperities must be deforming plastically or else are crushed when P_c is increased. Either plastic deformation or asperity crushing will increase the contact area and thus decrease the amount of surface area available for P_f to work against, in addition to increasing the flow tortuosity. Thus lowering the P_f value apparently permits non-recoverable surface damage. The permeability can be recovered only if the joint or crack aperture is increased.

Permeability hysteresis within whole rock is probably a result of irrecoverable damage done to bridging material between grains and crack walls. Sprunt & Brace [11] have shown that pressure produces such damage in granite. Feves & Simmons [18] have shown that pressure cycling decreases the crack porosity substantially. If pore pressure is decreased and cracks close down, raising the pore pressure to its initial value may not be sufficient to wedge the cracks open again. If the test is performed in reverse by first raising the pore pressure, the cracks will stay open and no damage is expected. Zoback's results [12] are not incompatible with ours in this respect.

One of the observations which we cannot so easily explain is found in Fig. 6. After completing a cycle of lowering and raising P_f , both were raised *simultaneously* (as in Fig. 2b). This had the apparently incongruous result of *raising* the permeability slightly, though it was still lower than the beginning of the previous cycle. We suggest that this may have been a result of not letting sufficient time elapse for P_f within the joint to come into equilibrium with the reservoir pressure. Thus $P_c - P_f$ may have been less within the joint than we measured outside of the sample column. Alternatively, it may be that when a joint is subjected to internal pressures not previously experienced, even when the $P_c - P_f$ value is constant, the contact area between asperities decreases.

CONCLUSIONS

Because the permeability of jointed rock is greater than unjointed, low porosity rock, fluid flow will be

confined essentially to joints and fractures in the rock. Large differences in permeability persist at least up to 2 kbars of pressure though the decrease in permeability with pressure is greater for joints than for whole rock. In addition, since joint surface roughness has an effect on the decline of permeability with pressure, some joints will probably be effective fluid conductors at even higher pressures. Eventually, however, a pressure is reached where jointed and unjointed rock become indistinguishable.

Changes in external (overburden) and internal (fluid) pressures have significant effects on the hydraulic properties of unjointed and jointed rock. It appears that these effects are similar but of different magnitude in whole as compared with jointed rock. Jointed rock is much more sensitive to pressure than whole rock. In a porous rock, flow is through interconnected pores and cracks. The mean cross sectional area along the flow path is much smaller than for a joint. In addition, the flow path length is much greater in whole rock. These two differences alone can account for the magnitude difference in permeability, but not for the fact that the permeability decreases more rapidly with pressure for jointed than for unjointed rock. Rather, it is apparently because the compressibility of jointed rock is much greater than for whole rock [4,6,19]. That is, the joint aperture closes more readily under pressure than cracks within the whole rock.

We find that external confining pressures produce greater changes than internal fluid pressures for jointed rock. In whole Barre granite, the relative changes are about equal. This may not be true of other rock types. One should be cautious when applying the term *effective stress* to jointed media. At least for the hydraulic properties of jointed rock it is *not* simply the difference between external confining and internal fluid pressures.

For flow through joints, a flat plate model of the joint seems inadequate and the stress history must be considered. Deviations from the flat model may occur under high stress or for very rough surfaces.

The stress history of both whole and jointed rock affects its hydraulic character. Increasing the mean normal stress to values higher than previously experienced will certainly lower the permeability. That is, raising the confining pressure or lowering the internal fluid pressure will result in lower permeabilities even when the original conditions are restored. This fact has obvious implications for oil field production and geothermal energy extraction schemes. If the internal fluid pumping pressures are allowed to drop, some subsequent decrease in hydraulic efficiency will ensue.

Finally, as there seems to be a substantial difference in the response of low porosity rock like granite and high porosity rock like sandstone to changes in fluid pressure, more work needs to be done to clarify the reasons for this difference. More jointed sandstones,

granites, and other rock types need to be tested. Joint surface topography changes need to be examined also, and as mentioned, we have begun such an investigation. *In situ* experiments, perhaps in mines, are also needed to help characterize further the differences in hydraulic response to changes in external and internal pressure.

Acknowledgements—The data in this report were collected as part of an on-going project supported by the Department of Energy under contract EY-S-02-4054 and the National Science Foundation under contract EAR-77-13000. T. Koczynski provided technical support. The manuscript was reviewed by D. Holcomb and K. Jacob. H. Murphy provided useful comments on an earlier version. Lamont-Doherty Contribution No. 2830.

Received 5 September 1978.

REFERENCES

1. Brace W. F., Walsh J. B. & Frangos W. T. Permeability of granite under high pressure. *J. geophys. Res.* **73**, 2225–2236 (1968).
2. Zoback M. D. & Byerlee J. D. The effect of microcrack dilatancy on the permeability of Westerly granite. *J. geophys. Res.* **80**, 752–755 (1975).
3. Summers R., Winkler K. & Byerlee J. Permeability changes during the flow of water through Westerly granite at temperatures of 100°–400°C. *J. geophys. Res.* **83**, 339–344 (1978).
4. Pratt H. R., Swolfs H. S., Brace W. F., Black A. D. & Handin J. W. Elastic and transport properties of an *in situ* jointed granite. *Int. J. Rock Mech. Min. Sci. & Geomech. Abstr.* **14**, 35–45 (1977).
5. Witherspoon P. A., Amick C. H. & Gale J. E. Stress-flow behavior of a fault zone with fluid injection and withdrawal, Report No. 77-1, Dept. of Materials Science and Mineral Engineering, University of California—Berkeley (1977).
6. Brace W. F. A note on permeability changes in geologic material due to stress. *Proc. of Conference II: Experimental Studies of Rock Friction with Application to Earthquake Prediction*. U.S.G.S., Menlo Park, CA (1977).
7. *International Critical Tables*, (Edited by Washburn E. W.). Vol. II, p. 146. McGraw-Hill, New York (1927).
8. Bridgeman P. W. The effect of pressure on the viscosity of 43 pure liquids. *Proc. Am. Acad. Arts Sci.* **61**, 57–99 (1926).
9. Snow D. T. A parallel plate model of fractured permeable media. Ph.D. Thesis, University of California—Berkeley (1965).
10. Norton D. & Knapp R. Transport phenomena in hydrothermal systems: the nature of porosity. *Am. J. Sci.* **277**, 913–936 (1977).
11. Sprunt E. & Brace W. F. Some permanent structural changes in rock due to pressure and temperature. *Proc. 3rd Cong. ISRM* Vol. IIA, 524–529, Denver, CO (1974).
12. Zoback M. D. High pressure deformation and fluid flow in sandstone, granite and granular materials. Ph.D. Thesis, Stanford University (1975).
13. Iwai K. Fundamental studies of fluid flow through a single fracture. Ph.D. Thesis, University of California—Berkeley (1976).
14. Bowden F. P. & Tabor D. *The Friction and Lubrication of Solids* Vol. I. Clarendon Press, Oxford (1950).
15. Douglas P. M. & Voight B. Anisotropy of granites: A reflection of microscopic fabric. *Geotechnique* **19**, 376–398 (1969).
16. Mordecai M. & Morris L. H. An investigation into the changes of permeability occurring in a sandstone when failed under triaxial stress conditions. *12th Symp. Rock Mech., Rolla, MO.* (Edited by Clark G. B.). Chap. 11. Port City Press, Baltimore, MD (1971).
17. Nelson R. A. & Handin J. Experimental study of fracture permeability in porous rock. *Am. Ass. Pet. Geol. Bull.* **61**, 227–236 (1977).
18. Feves M. & Simmons G. Effects of stress on cracks in Westerly granite. *Bull. Seism. Soc. Am.* **66**, 1755–1765 (1976).
19. Daw G. P., Howell F. T. & Woodhead F. A. The effect of applied stress upon the permeability of some Permian and Triassic sandstones of northern England. *Proc. 3rd Congr. ISRM* Vol. IIA, 537–542, Denver, CO (1974).